Enspect: a Complete Tool using Modeling and Real Data to Assist the Design of Energy Harvesting Systems

Nick F. Tinsley, Stuart T. Witts, Jacob M. R. Ansell, Emily Barnes,
Simeon M. Jenkins, Dhanushan Raveendran, Geoff V. Merrett, Alex S. Weddell
Electronics and Computer Science, University of Southampton, UK
{ntinsley, switts, jansell, ebarnes, sjenkins, draveendran, gvm, asw}@ecs.soton.ac.uk

ABSTRACT

Energy harvesting is the process by which energy (often solar or thermal) is captured from the environment to power small electronic devices. The available energy is often spatially and temporally variant, which makes the potential for power generation difficult to estimate. In this paper we present Enspect: a complete tool which comprises a portable logger that collects real environmental data, and analysis software which models the performance of energy harvesting systems in that application. It enables components to be chosen and exchanged, and models long-term system behavior. It has been demonstrated with photovoltaic and thermoelectric devices, but its modular design means that it can be expanded to include other harvesting types.

Categories and Subject Descriptors

B.8.2 [**Hardware**]: Performance and Reliability—*Performance Analysis and Design Aids*

General Terms

Algorithms, Design, Measurement

Keywords

energy harvesting, design tools, modeling

1. INTRODUCTION

Energy harvesting is the conversion of ambient energy from the environment into electricity, usually for low-power electronic devices [3]. Energy availability varies both temporally and spatially; to deliver a reliable power supply, systems must be designed with this in mind, and also take account of the dynamics of the application load. For example, decisions must be made about the type, size, and topology of energy harvesting systems, as well as energy storage devices, and the power consumption profile of the load.

Two prominent portable tools, Ekho [8] and SunaPlayer [6], have been developed which aid in the design of systems through the capture and use of real data on energy availability. Ekho [8] records the voltages and currents produced by energy harvesters so their electrical properties can retrospectively be emulated. As Ekho only records power characteristics of the particular measured device, it is unable to estimate energy availability from different harvesters. For example, the chemistry of a photovoltaic (PV) cell affects its sensitivity to the intensity and spectral composition of light [16]. This means that it is not feasible to use the data collected using one PV cell chemistry to estimate the power output of a different cell under the same conditions. Furthermore, Ekho's output is controlled by a microcontroller and will not react instantly to changes; energy must be buffered in a storage device (therefore smoothing the load dynamics).

To resolve the latter limitation of Ekho, SunaPlayer [6] uses an analog non-linear device with characteristics close to those of a PV cell, allowing it to respond more accurately. However, SunaPlayer is only designed for evaluating and debugging solar panel-driven systems. A sensor records the ambient light intensity which can be used by SunaPlayer to select an appropriate I-V curve from solar panel traces collected either experimentally or from datasheets. This system does not use an analytical model for estimation of energy availability, but can aid in the selection of the most appropriate PV cell or panel using its corresponding I-V curve.

LightBox is the first portable irradiance measurement tool that considers the spectral composition of incident light [16]. Models calculate the total available environmental energy and estimate the total energy harvested by a particular PV cell chemistry. However, the tool achieves this by classifying the light source (e.g. LED, fluorescent or incandescent) through spectral composition and deciding whether a crystalline silicon or amorphous silicon cell is most suitable. The performance of specific PV cells (rather than broader chemistries), and non-PV harvesters, cannot be predicted.

To improve on the aforementioned tools, we present Enspect, which: **(1)** models the performance of energy harvesters (Section 2), **(2)** enables the collection of real environmental data using a portable tool (Section 3.1), and **(3)** allows system components to be exchanged and for their effect on system operation to be simulated (Section 3.2). This simplifies the process of designing energy harvesting systems. It has been tested to evaluate various scenarios (Section 4). The tool's modular design also means that other types of energy harvesters can be considered in the future. The tool's embedded software, schematics, PCB designs and analysis tool software are open-source and available for download [15].

ENSsys'15, November 1, 2015, Seoul, South Korea..

DOI: http://dx.doi.org/10.1145/2820645.2820648.

2. MODELLING ENERGY AVAILABILITY

To estimate the power output from a harvester, the relationship between input stimulus and output power needs to be accurately modelled. As a proof-of-concept, two types of energy harvester are considered and reported in this paper: PV cells and thermoelectric generators (TEGs). Both energy harvester models use environmental data and parameters gathered from datasheets and through experimentation, but for brevity a simplified TEG model is reported.

2.1 Photovoltaic Cell Model

Equivalent circuit models are commonly used to represent the performance of PV cells. Only environmental variables that produced a significant effect are included in the model; these include the light intensity and surface temperature of the cell. The effects of wind and humidity on the cell are ignored as it has been proven that neither significantly affect the power output [4, 10]. The output characteristic of a PV cell in the dark resembles the exponential characteristic of a diode, so a full PV cell can be modelled by a current source, diodes, and both shunt (R_p) and series (R_s) resistances [5]. These characteristics can either be calculated using values from the PV cell's datasheet, or through experiment.

Equivalent circuit models typically include either one or two diodes [9, 13, 17]. One-diode models are less accurate at low values of irradiation, e.g. 100W/m^2 (equivalent to 10% of the nominal sunlight intensity on a bright day), as they do not model carrier recombination [5]. The two-diode model is well-documented, however some equivalent circuit parameters, notably R_s and R_p, must be derived from others. Some texts simply estimate these resistances [13], but we sought a model that would be able to more accurately determine them with a method proven to be effective. The single-diode model presented in [17] demonstrates a novel method of calculating the equivalent circuit parameters from datasheet parameters. This method involves a curve-fitting technique to determine the equivalent circuit resistances. The technique was then expanded into a two-diode model by Ishaque [9]. This forms the basis for our own PV cell model, which improves its performance at very low light levels.

In our model, R_p and R_s are determined by simultaneously increasing the two values [9]. The algorithm aims to find where the experimental and predicted Maximum Power Point (MPP) on the I-V curves match by comparing the difference between the two values. When the difference is below a certain tolerance, an appropriate simulated curve has been found. This tolerance must be carefully selected; too low and the MPP will be found with low accuracy, too high and the MPP will not be found as the algorithm continues to iterate beyond the acceptable values. Our solution to this uncertainty is to use a variable convergence tolerance: when R_s overshoots its acceptable value, R_p tends towards minus infinity. The tolerance is therefore reduced when R_p falls below zero, and the process restarts. This method preserves accuracy while minimising calculation times.

As this device is intended to model the performance of PV modules in both indoor and outdoor environments, it was vital that the model produced accurate results with a range of light levels. The initial model deviates from the actual performance at levels below 50W/m^2 because the value of R_p is assumed to be a constant, but experimental data shows this is not the case [14]. For all cells, the value of R_p increases with decreasing irradiance, although the cell chemistry can affect the rate of this increase [2, 14]. The dashed lines in figures 1 and 2 demonstrate this problem, using a simulation of Alta Devices' GaAs "Standard Cell" compared against its datasheet graphs [1]. The curve is acceptable at high irradiances (Figure 1) but deteriorates severely at indoor light levels (Figure 2) where the shape becomes unrecognisable.

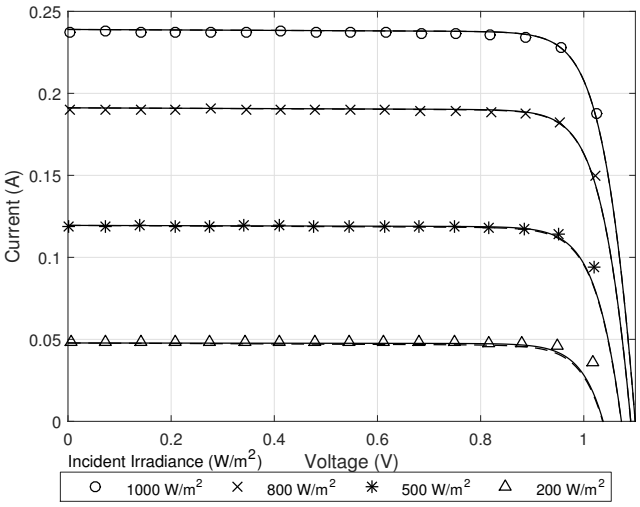

Figure 1: Effect of adjusting R_p at high irradiances. Points: original datasheet measurements (from [1]); solid: corrected model prediction; dashed: uncorrected model prediction.

Developers of commercial simulation software [14] propose an exponential relationship between increasing R_p and decreasing irradiance. However, our testing found that a power law provided a much better fit, particularly in regions of very low (<10W/m^2) irradiance, as it allowed R_p to tend to infinity rather than to a particular intercept. This modification, applied to R_p at irradiance G (where G_{ref} is the irradiance at which the original value of R_p was determined), is therefore shown in equation (1). From the initial condition of the uncorrected R_p shown in equation (2), it is then possible to express the relation with a single parameter, β, as shown in equation (3). This fit is important because it allows an arbitrary reference irradiance to be included which can be used to scale datasheet values that may not be referenced to standard test conditions. By fitting a curve to the data given in [14], a value of $\beta = 0.84$ was calculated.

$$R_p = a\left(\frac{G}{G_{ref}}\right)^{-\beta} \tag{1}$$

$$\text{When } G/G_{ref} = 1,\ R_p = a(1)^{-\beta} \tag{2}$$

$$\text{So } a = \frac{R_p}{1^{-\beta}} = R_p \tag{3}$$

Tests were again conducted with reference to the Alta Devices cell and the results showed improved curve matching (solid line in Figure 2), giving much better agreement with the datasheet. Despite the cell being different from those tested in [14], the same exponent of $\beta = 0.84$ in the adjustment process still allowed close match, as can be seen in Figure 2. In addition to the GaAs Alta Devices cell, the model has also been verified against the mono- and multi-

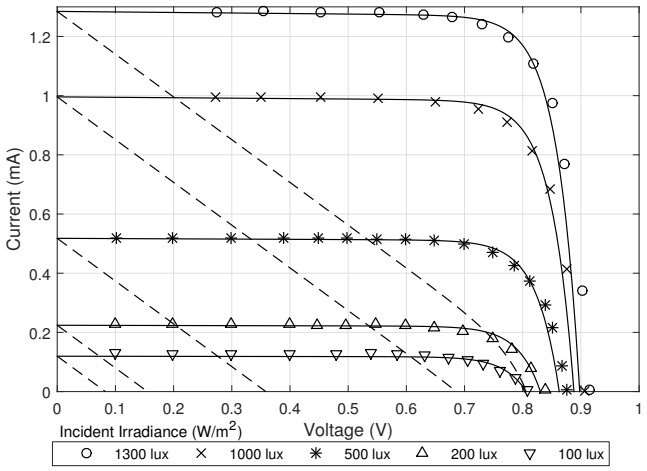

Figure 2: Effect of adjusting R_p at low irradiances. Points: original datasheet measurements (from [1]); solid: corrected model prediction; dashed: uncorrected model prediction.

crystalline Si cells discussed in [9], as well as the amorphous silicon Cymbet CBC-PV-02 [7] for which the model produced an I-V curve with average percentage error of 1.4% against experimental values. This demonstrates that the adjustment can be applied generally, irrespective of cell type.

2.2 Thermoelectric Generator Model

The TEG model considered the Ortiz-Rivera equations [12], which relate the thermal properties of the device to its electrical characteristics. A minimum of two measurements of open circuit voltage and short circuit current values need to be taken at different temperature gradients, with the hot- and cold-side temperatures of the TEG also recorded. These values can be acquired from a TEG datasheet, or found by experiment. From these values, an I-V curve is produced which is then extrapolated for different hot-side temperatures. This model makes several assumptions that could reduce accuracy; for example, heat extraction can cause the surface to cool, but the model assumes a heat source of infinite capacity which could cause overestimation of energy availability. The modelled device is also assumed to have a constant temperature gradient. This does not take into account the cold-side heat dissipation, Seebeck coefficients, or other material properties that can cause subtle differences in the functionality of the device. As described in Section 3.2, the tool is modular and allows models to be exchanged.

To verify the accuracy of the model, energy availability estimations were compared with real-world test results. A Micropelt TEG module [11] was characterised using the parameters given on its datasheet. The maximum power was calculated for hot-side temperatures between 40 and 100°C, and compared with experimental results [11]. The results (Figure 3) show a good agreement, with a 2.6% mean error.

3. ENERGY AVAILABILITY TOOL

To enable environmental data to be captured, a portable tool has been produced. This data is processed by the analysis tool, which uses models to predict the performance of energy harvesters and the rest of the system. The tool's embedded software, schematics, PCB designs and analysis tool software are open-source and available for download [15].

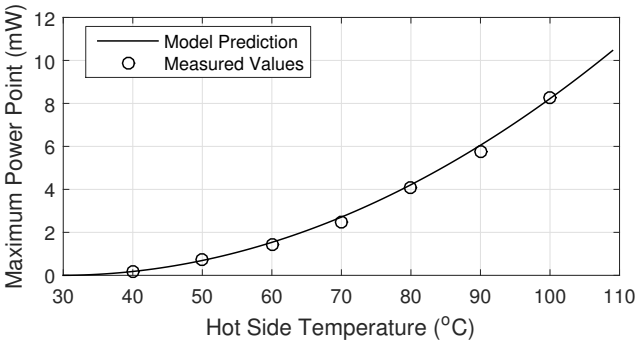

Figure 3: Simulation of maximum power output from Micropelt TEG module [11] over a range of temperatures compared to real-world measurements.

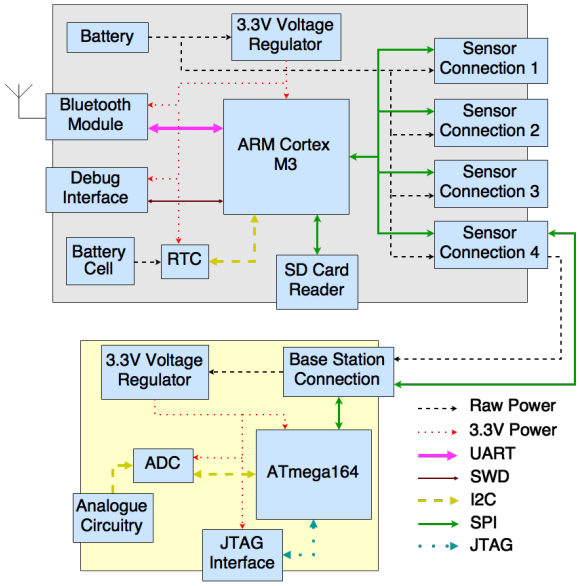

Figure 4: Block diagram of the data collection unit (DCU) and PV sensor module.

3.1 Hardware and Embedded Software

The data collection unit (DCU) enables the collection of data on in-situ environmental energy availability. Its modular architecture (Figure 4) means that various sensor modules may be connected[1]. It accommodates up to four modules simultaneously, so that multiple energy harvesting methods can be assessed. Furthermore, it allows sensors to be placed in precise and different locations to other sensor modules; for example, two photovoltaic sensor modules could be placed at different positions and angles.

The DCU coordinates the data collection process, requesting samples from the sensor modules and storing the results. Data is stored on an SD card, allowing new memory to be inserted in the field if necessary. It incorporates a Blue-

[1]A minor firmware update on the DCU would be required to allow it to recognise new module(s).

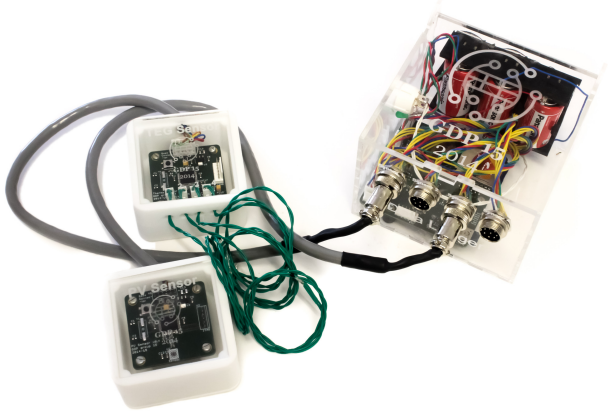

Figure 5: The DCU with two sensor modules (PV and TEG) attached.

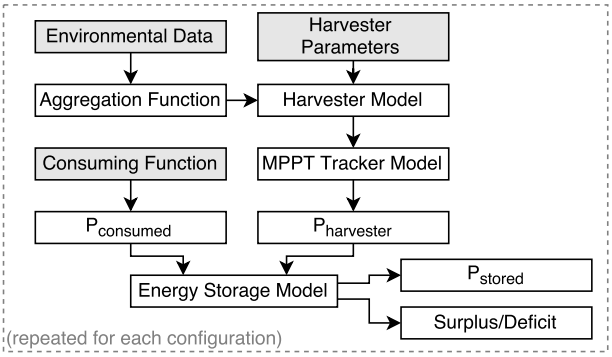

Figure 6: Analysis tool architecture and components.

tooth link, which is used for device configuration and to view real-time sensor data (the system can also be set up with a configuration file on the SD card). The overall system is battery-powered, with every module incorporating a 3.3V linear regulator to ensure supply stability.

Each sensor module is intelligent and designed to collect and pre-process all data needed to model a particular energy harvesting method. They incorporate sensors, analogue circuitry, ADCs and a microcontroller. On-module pre-processing means that module sample rates are not dependent on the speed of the bus or other latencies associated with data transfer to the DCU. For example, if the system were expanded to include a vibration sensor, the sensor module would sample accelerometer data at a high frequency (at least the Nyquist rate e.g. 100 Hz for a 50 Hz vibration source) but may pre-process this and only send spectral data to the DCU once per second. Future modules may require real-time signal processing beyond the capabilities of the DCU's microcontroller. This architecture maintains flexibility and minimizes the DCU's workload.

For this initial system, two sensor modules were developed: for collecting data to model PV cells and TEG performance. Future modules could be created that collect data to model wind, RF, vibration, or other harvesting methods. The PV sensor module measures the ambient temperature, ambient light level, and red/green/blue/infrared light levels (the latter is not used in the version of the PV model presented in Section 2). The TEG sensor module collects temperature data using thermistors; the thermistors are on leads so that they can be placed on the TEG's surfaces. Sensor readings are aggregated by each module into a data packet which is sent back to the DCU when requested. A block diagram of the PV sensor module architecture is shown in Figure 4. Housings were made for the DCU and for the photovoltaic and thermoelectric sensor modules in order to increase durability. The final device is shown in Figure 5.

3.2 Analysis Tool

The analysis tool serves two main purposes: firstly, to enable configuration of the DCU via Bluetooth, and secondly to interpret the data measured by the DCU to assist in the design of energy harvesting systems. The user interface was developed in MATLAB along with the underlying modelling algorithms, and allows the user to make changes to the system and observe their effects.

The complete system model implemented in the tool (Figure 6) takes environmental data and harvester parameters to model the electrical performance of the harvester. The dynamics of the MPP tracking unit (if any) are also modelled; this then generates an estimate of the harvester's output power ($P_{harvester}$). Similarly, the dynamics of the load are represented by the consuming function, which generates an estimate of the power consumed by the load ($P_{consumed}$). This is fed into the energy storage model, outputting an estimate of the power stored. It can also monitor the power *surplus* or *deficit*; this is when power is generated but wasted as the storage device is full, or when the load demands power which cannot be supplied as it is completely depleted.

The tool comes with built-in implementations for all components, except for the load function (which is specified by the user in the form of a MATLAB command). This may be set to a constant power draw, or a function e.g. a square wave which emulates the power consumption profile of a device which periodically wakes up for a short time to perform some operation before sleeping. The application is capable of working with multiple data sets to either compare between them, e.g. recordings in different locations, or to aggregate them, e.g. to obtain an 'average' 24-hour period from data recorded over several days.

$$P(t) = P_{harvester}(t) + P_{stored}(t) - P_{consumed}(t) \quad (4)$$

At time t, $P_{harvester}$ is the output of the energy harvester under simulation as determined by the relevant model, $P_{consumed}$ is the value of the consuming function, and P_{stored} is the flow of power in or out of the battery. P_{stored} acts to reduce the result of equation (4) to zero by either giving a negative power to represent charging (where there is excess power and the battery is not already fully charged), or a positive value to represent discharging to support the load (if there is sufficient charge at t to do so). If the final result of $P(t)$ is greater than zero, then there is a *surplus* of power which was not used to either power the load or charge the battery, and hence was wasted. If $P(t)$ is less than zero there is a *deficit*, indicating a time where the system could not power the load. This quantity is useful as it indicates whether elements of the system are under- or over-sized. In the case where a sys-

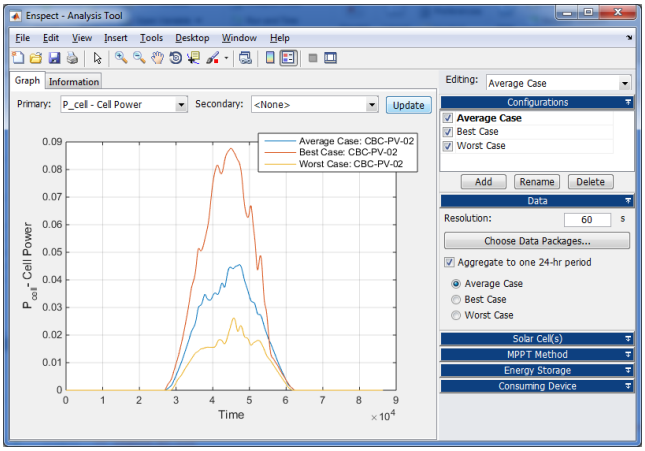

Figure 7: Analysis tool simulating a simple solar energy harvesting system, predicting the output from one cell with average, best, and worst case data.

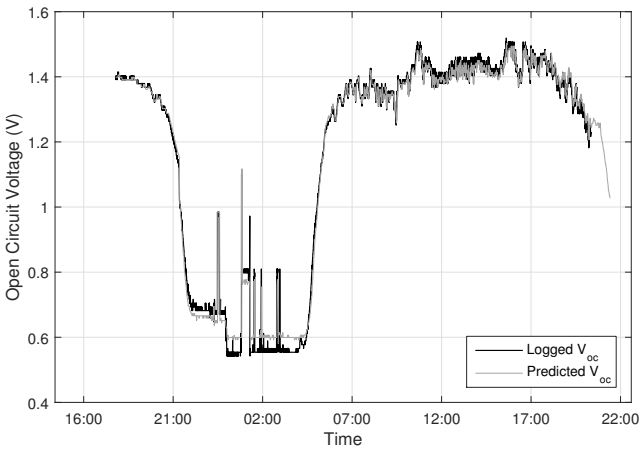

Figure 8: Test of Enspect DCU and analysis tool, comparing the predicted V_{oc} to actual measured values.

tem goes into both surplus and deficit during a test period, this indicates that the capacity of the storage device should be increased. For a system which only goes into surplus, this shows that the energy harvester may be over-sized, and for one that only goes into deficit this indicates that the energy storage device may be under-sized.

A modular architecture is used whereby each of the components can be swapped out for a different implementation, allowing for alternative harvester, power conditioning circuit, or energy storage models to be incorporated at a later stage. For example if the user wished to use a supercapacitor instead of a battery, they would just need to implement the methods used to charge and discharge accordingly to represent the desired characteristic. Every setting in the model is encapsulated in a 'configuration' object, and an unlimited number of configurations can be simultaneously manipulated in the tool. This allows for any feature to be compared – e.g. input data could be set differently in each configuration to compare different locations or times of day in order to decide system placement, or several battery capacities could be evaluated to find an appropriate one.

As most electronic circuits require a constant voltage, it was therefore assumed that a Buck/Boost power converter, battery, or voltage regulator device was present which would regulate the output to deliver a consistent voltage to the load. This follows the example of other energy harvesting prediction systems [11]. An example simulation with multiple configurations for a photovoltaic system is shown in Figure 7. In this example, the tool has been supplied with 7 days of irradiance data, and three different configurations have been created with different aggregation settings. This produces three lines, showing power on average, best-, and worst-case 24-hour periods.

4. RESULTS AND ANALYSIS

A large range of results are available from the analysis tool in both graphical and tabular form, including graphs of output power, with and without a MPP tracker device and the voltage and current at which this point occurs. Statistics such as the average irradiance and percentage time the device was sufficiently powered are also available. Finally, the analysis tool is also able to aid selection of PV cell chemistry by estimating the relative efficiency of cell chemistries at the recorded irradiances. A selection of these are illustrated in this section to demonstrate the use of the tool.

To verify the effectiveness of both the analysis software and data collection hardware, the system was left to run on a windowsill for over 24 hours with the PV sensor attached. Meanwhile, the CBC-PV-02 amorphous solar cell was attached to a data logger which logged the open circuit voltage for the same period. The prediction of V_{oc} from the simulation based on the recorded data was then compared to the real result, as shown in Figure 8.

The results given by the tool can help to find a suitable combination of energy harvester and battery, which will now be explored with a brief example. Figure 9 shows an undersized system. The tool is simulating two candidate solar cells, and has averaged 7 days of data to give a 24-hour period for evaluation. The load has been set as a square wave to model a duty-cycled sensor node that is in a high-power state (40mA) for 10 minutes every hour, and a low-power state (1mA) otherwise – producing the periodic sharp drops followed by slower falls in the battery charge level graph. In this case we can see that both solar cells are providing plenty of power during the peak sunlight period, however a large surplus is shown, meaning that most of this power is wasted, neither being used by the load nor stored in the battery. Conversely, during the dark periods, a deficit is shown, indicating there is not enough energy stored in the battery. The battery charge fraction line shows that the battery charges to full capacity in the middle of the day, wasting the rest of the solar power, then discharges to zero before the next sunrise. This indicates that the battery capacity is insufficient.

After increasing the capacity from 4.5mAh to 15mAh (but retaining the same system configuration and initial charge level of 3mAh), the simulation was re-run to give Figure 10. There is now no surplus, indicating that no energy is wasted in the system, and the battery can now support the device after 22:00, unlike in Figure 9. We can also see that the CBC-PV-02 cell charges the battery considerably higher in the daylight period, and therefore likely to be a better choice.

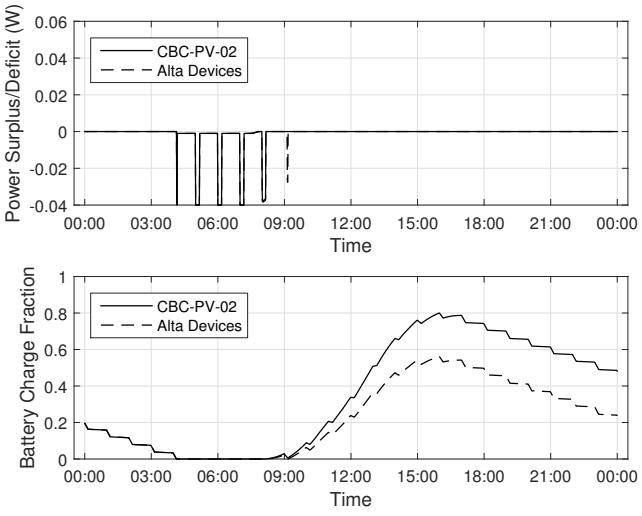

Figure 10: Improved system design showing no surplus and no deficit after the daylight period.

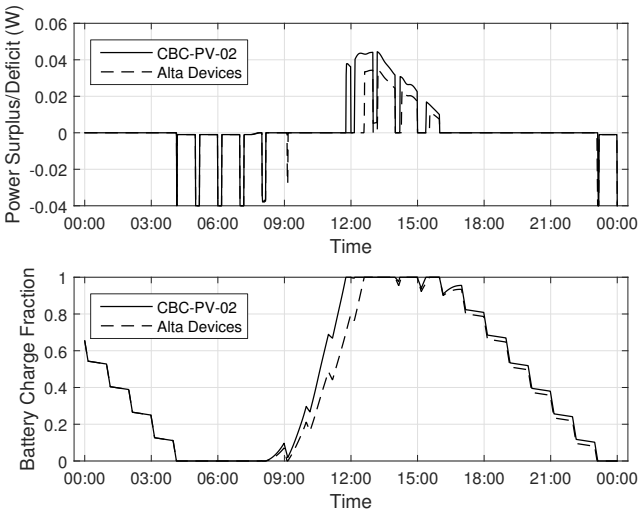

Figure 9: Simulation with an under-sized battery: a surplus where power is wasted as the battery was full, and deficit where the load was not able to be powered.

5. CONCLUSION

This paper has presented Enspect, a tool for assisting in the design of energy harvesting systems. It enables the collection of real data, and uses device models incorporated into its analysis software to enable the behavior of energy harvesting systems and their load to be simulated over an extended time period. It assists with design decisions such as the selection of an appropriate energy harvester, power conditioning circuit, and storage device. The tool is flexible and can be expanded to cover a wide range of harvesting types. The system has been demonstrated with TEG and PV sensor modules, and through a novel PV cell model which is accurate across a very wide range of light intensities is able to predict PV cell outputs with a mean error of 1.4%. The tool is open-source and available for download [15].

6. REFERENCES

[1] Alta Devices. Single solar cell, 2014. [Online; Accessed December 2014].

[2] D. Batzner, A. Romero, H. Zogg, and A. Tiwari. CdTe/Cds solar cell performance under low irradiance. 2001. 17th EC PVSEC, Munich.

[3] S. Beeby and N. White. *Energy Harvesting for Autonomous Systems Characteristics*. Artech House, Inc, Norwood, MA, USA, 2009.

[4] T. Bhattacharya, A. Chakraborty, and K. Pal. Effects of ambient temperature and wind speed on performance of monocrystalline solar photovoltaic module in Tripura, India. *Journal of Solar Energy*, (5):5, 2014.

[5] G. Bhuvaneswari and R. Annamalai. Development of a solar cell model in MATLAB for PV based generation system. pages 1–5, 2011. INDICON, Hyderabad.

[6] S. Bobovych, N. Banerjee, R. Robucci, J. P. Parkerson, J. Schmandt, and C. Patel. In *SunaPlayer: high-accuracy emulation of solar cells*, pages 59–70, 2015. European Photovoltaic Solar Energy Conference and Exhibition, Barcelona.

[7] Cymbet. CBC-PV-02 photovoltaic cell, 2012. [Online; Accessed December 2014].

[8] J. Hester, T. Scott, and J. Sorber. Ekho: realistic and repeatable experimentation for tiny energy-harvesting sensors. pages 1–15, 2014. SenSys ACM Conference on Embedded Network Sensor Systems, Memphis, TN.

[9] K. Ishaque, Z. Salam, and H. Taheri. Accurate MATLAB simulink PV system simulator based on a two-diode model. *Journal of Power Electronics*, 11(2):179–187, 2011.

[10] S. Mekhilef, R. Saidur, and M. Kamalisarvestani. Effect of dust, humidity and air velocity on efficiency of photovoltaic cells, 2012. [Online; Accessed 30 October 2014].

[11] Micropelt. TE-Power NODE: Self-sufficent wireless sensor system thermoharvesting explorer, 2011. [Online; Accessed January 2015].

[12] E. Ortiz-Rivera, A. Salazar-Llinas, and J. Gonzalez-Llorente. A mathematical model for online electrical characterization of thermoelectric generators using the P-I curves at different temperatures. *Applied Power Electronics Conference and Exposition*, pages 2226–2230, 2010.

[13] M. C. D. Piazza and G. Vitale. Matlab/Simulink simulation of PV electrical characteristics. 2013.

[14] PVSyst. PV module - Rshunt exponential behavior vs irradiance, 2014. [Online; Accessed January 2015].

[15] Removed for blind review. Enspect free resources online. URL Removed for blind review, 2015. [Online].

[16] J. Sarik, K. Kanghwan, M. Gorlatova, I. Kymissis, and G. Zussman. More than meets the eye - a portable measurement unit for characterizing light energy availability. pages 387–390, 2005. Global Conference on Signal and Information Processing, Austin, TX.

[17] M. G. Villalva, J. Gazoli, and E. Filho. Comprehensive approach to modelling and simulation of photovoltaic arrays. *Power Electronics*, 24(5):1198–1208, March 2009.